

Supplementary Materials for
**Activation of endogenous retroviruses and induction of viral mimicry by
MEK1/2 inhibition in pancreatic cancer**

Alice Cortesi *et al.*

Corresponding author: Gioacchino Natoli, gioacchino.natoli@ieo.it

Sci. Adv. **10**, eadk5386 (2024)
DOI: 10.1126/sciadv.adk5386

The PDF file includes:

Figs. S1 to S7
Legends for tables S1 to S6

Other Supplementary Material for this manuscript includes the following:

Tables S1 to S6

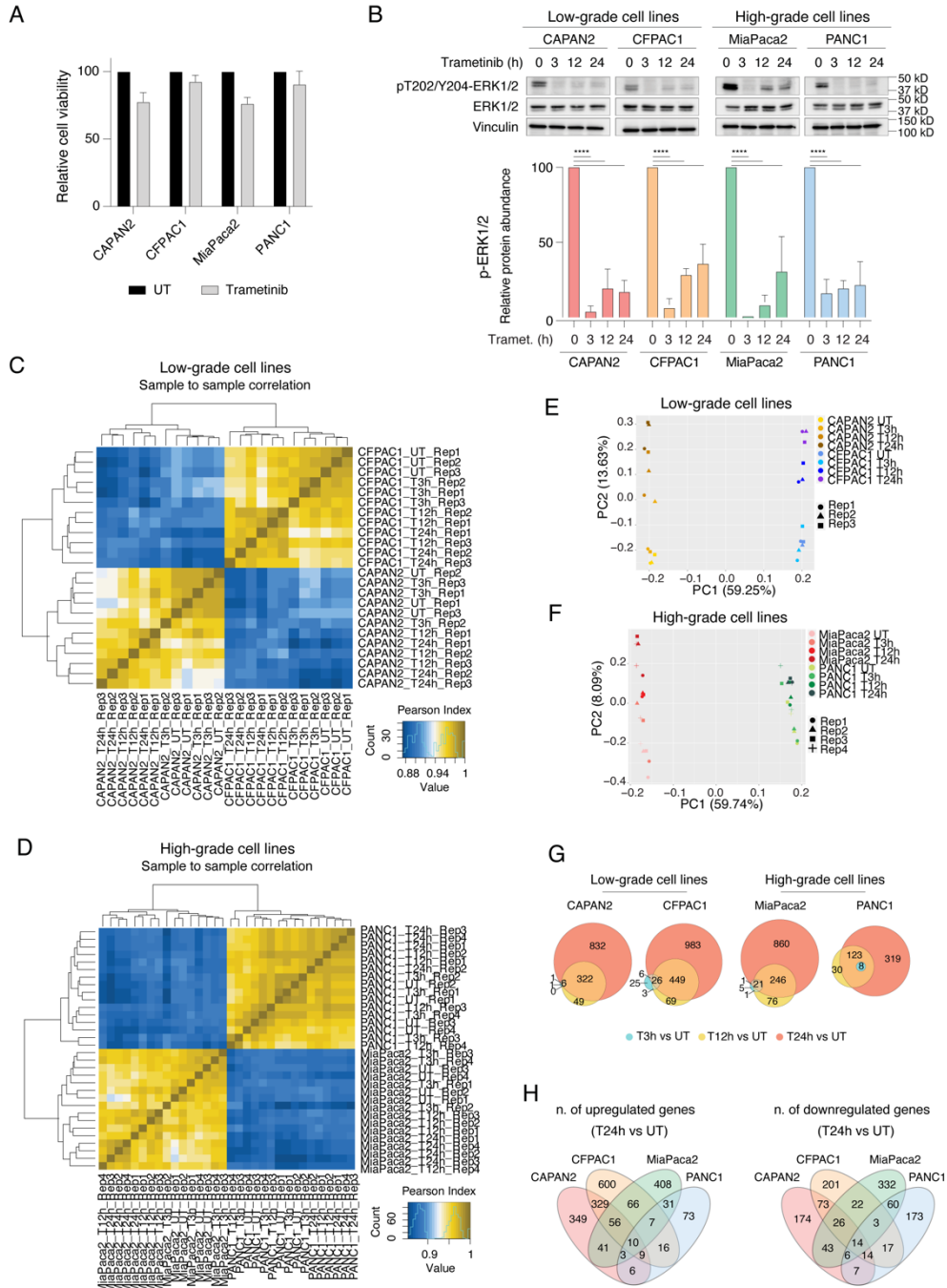


Figure S1. Differential gene expression in Trametinib-treated PDAC cells.

A) Viability of PDAC cell lines after treatment with 20 nM Trametinib for 72h. The percentage of viable cells was calculated relative to the corresponding untreated cells. $n=3$ independent biological replicates. Means \pm S.D. are shown.

B) ERK1/2 phosphorylation in Trametinib-treated PDAC cell lines.

Upper panel: Western blot analysis of pT202/Y204-ERK1/2 and total ERK1/2 abundance in low-grade and high-grade PDAC cell lines during the Trametinib treatment time course

for the indicated times. Vinculin is shown as loading control. Molecular weight markers are indicated on the right. The experiment is representative of n=4 independent experiments. Bottom panel: Quantification of pERK1/2 protein levels in the western blot analysis, normalized based on the vinculin loading control and relative to the corresponding untreated cells. n=4 independent biological replicates. Means \pm S.D. are shown. Significance was assessed using Two-way ANOVA and indicated as follows: **** $p \leq 0.0001$.

C-D) Hierarchical clustering heatmaps showing correlation of RNA-seq samples in low-grade and high-grade PDAC cell lines. n=3 independent biological replicates are shown.

E-F) Principal Component Analyses of RNA-seq data from low-grade and high-grade PDAC cell lines.

G) Venn diagrams showing the overlap between genes upregulated at different time points in each tested cell line.

H) Venn diagrams showing the overlap of upregulated and downregulated genes among all PDAC cell lines tested after 24h Trametinib treatment.

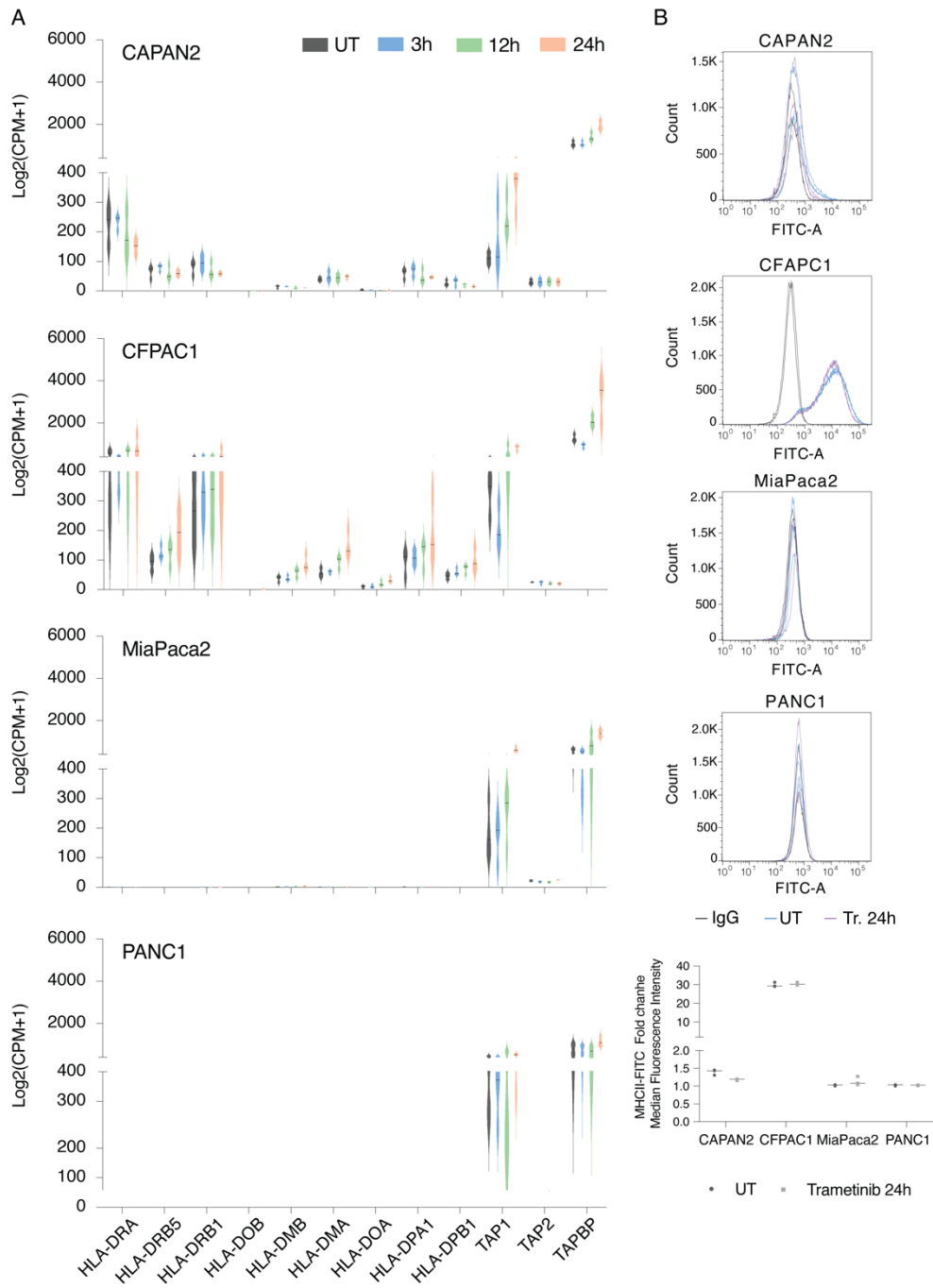


Figure S2. Effects of Trametinib treatment on the expression of components of the antigen presentation machinery.

A) RNA-seq data counts showing the expression of selected MHC-II genes and genes encoding components of the ER-associated TAP (transporter associated with antigen processing) in low-grade and high-grade PDAC cell lines after Trametinib treatment.

Data are reported as the log of Count Per Million (CPM) after TMM-normalization with EdgeR.

B) MHC class II expression in Trametinib-treated PDAC cell lines.

Top panels: Flow cytometry overlay histograms showing FITC signals for IgG-Alexa Fluor 488 and pan MHC-II-FITC staining in low-grade and high-grade PDAC cell lines after treatment with Trametinib or vehicle for 24h.

Bottom panel: Median fluorescence intensity of MHC-II based on anti-HLA-DR, DP, DQ-FITC staining in low-grade and high-grade PDAC cell lines after treatment with Trametinib for 24h. Data shown are normalized on IgG-Alexa Fluor 488. n=3 independent biological replicates.

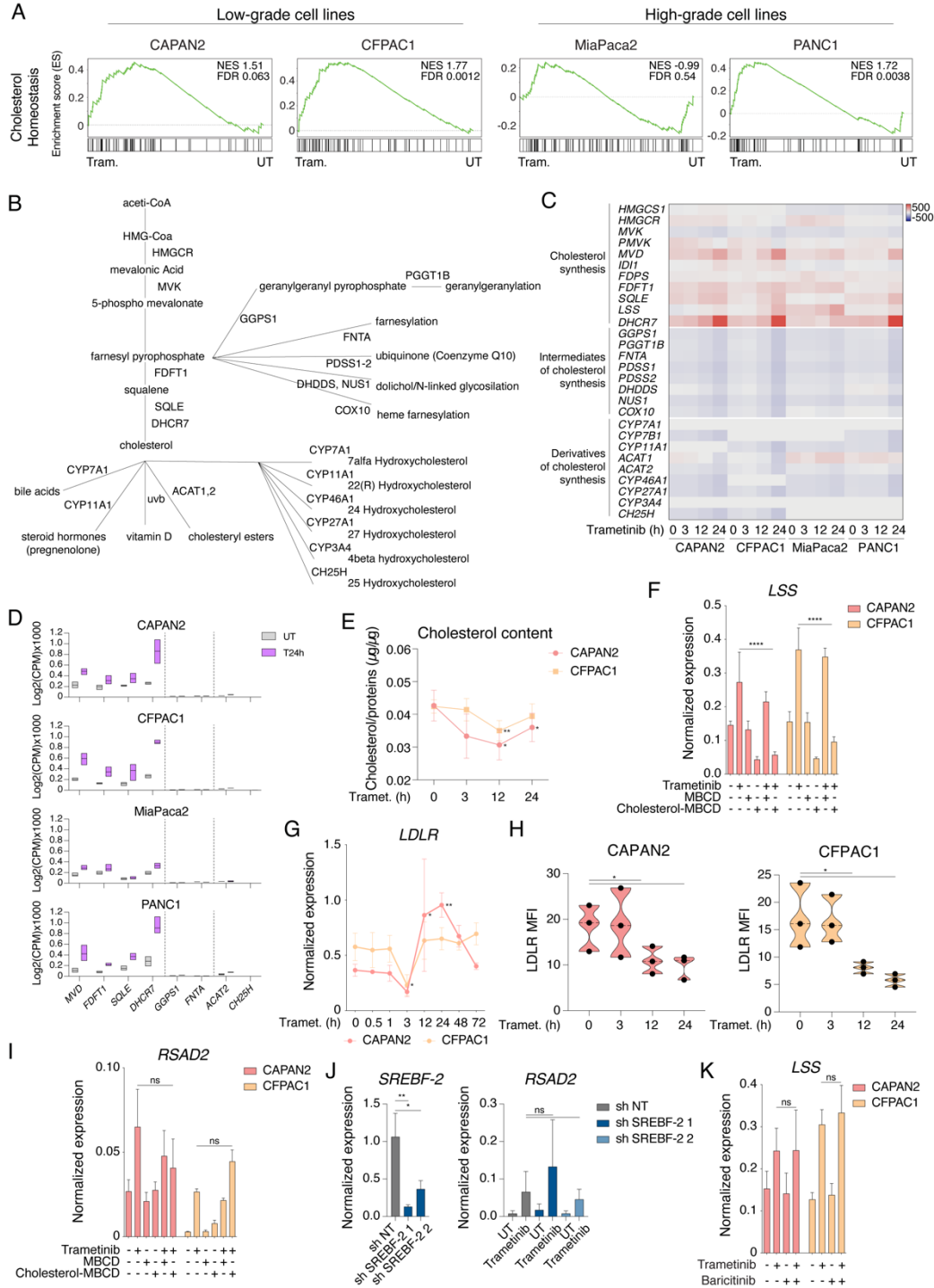


Figure S3. Activation of cholesterol synthesis by Trametinib and its relationship with the IFN program.

A) GSEA plots showing the differential enrichment of the cholesterol homeostasis gene signatures in low-grade and high-grade PDAC cell lines treated with Trametinib for 24h relative to untreated cells.

B) Schematic representation of the cholesterol biosynthetic pathway, showing pathway intermediates and derivatives, as well as the principal enzymes involved in each reaction.

C) Expression levels of genes encoding for the main cholesterol synthesis genes and in low-grade and high-grade PDAC cell lines after Trametinib treatment.

D) RNA-seq data counts showing the expression of some representative genes of the cholesterol biosynthetic pathway in low-grade and high-grade PDAC cell lines after treatment with Trametinib or vehicle for 24h. Data are reported as the log of Count Per Million (CPM) after TMM-normalization with EdgeR.

E) Quantification of cholesterol abundance in low-grade cell lines after Trametinib treatment. Data shown are normalized on protein content. n=3 (CAPAN2) or 5 (CFPAC1) independent biological replicates. Means \pm S.E.M. are shown. Significance was assessed using T-test and indicated as follows: * $p \leq 0.1$, ** $p \leq 0.01$.

F) Expression of the Lanosterol synthase (*LSS*) gene was measured by RT-qPCR in low-grade PDAC cell lines after treatment with Trametinib or/and MBCD or Cholesterol-MBCD for 24h. Values represent $2^{-\Delta Cq}$ relative to *CIORF43*. n=3 independent biological replicates. Means \pm S.D. are shown. Significance was assessed using two-way ANOVA and indicated as follows: **** $p \leq 0.0001$.

G) Expression of the Low-density lipoprotein receptor (*LDLR*) gene was measured by RT-qPCR in low-grade PDAC cell lines during the Trametinib treatment time course. Values represent $2^{-\Delta Cq}$ relative to *CIORF43*. n=3 independent biological replicates. Means \pm S.D. are shown. Significance was assessed using One-way ANOVA and indicated as follows: * $p \leq 0.05$, ** $p \leq 0.01$.

H) Mean fluorescence intensity of LDLR based on anti-LDLR-Phycoerythrin staining in low-grade PDAC cell lines after Trametinib treatment for the indicated times. Data shown are normalized on IgG-PE. n=3 independent biological replicates. Means \pm S.D. are shown. Significance was assessed using Two-way ANOVA and indicated as follows: * $p \leq 0.1$.

I) Expression of the IFN-stimulated gene *RSAD2* was measured by RT-qPCR in low-grade PDAC cell lines after treatment with Trametinib or/and MBCD or Cholesterol-MBCD for 24h. Values represent $2^{-\Delta Cq}$ relative to *CIORF43*. n=3 independent biological replicates. Means \pm S.E.M. are shown. Significance was assessed using Two-way ANOVA and indicated as follows: ns $p > 0.05$.

J) Left panel: RT-qPCR analysis of the *SREBF-2* gene mRNA in CFPAC1 bulk populations infected with lentiviral vectors expressing either a non-targeting (NT) shRNA or two different SREBF-2-targeting shRNAs. Values represent $2^{-\Delta Cq}$ relative to *CIORF43*. n=3. Means \pm S.D. are shown. Significance was assessed using One-way ANOVA and indicated as follows: * $p \leq 0.05$, ** $p \leq 0.01$. Right panel: Expression of the IFN-stimulated gene *RSAD2* was measured by RT-qPCR in CFPAC1 bulk populations of

WT or SREBF-2 depleted cells after treatment with Trametinib or vehicle for 24h. Values represent $2^{-\Delta Cq}$ relative to *CIORF43*. n=3 independent biological replicates. Means \pm S.D. are shown. Significance was assessed using One-way ANOVA and indicated as follows: ns $p > 0.05$.

K) Expression of the *LSS* gene was measured by RT-qPCR in low-grade PDAC cell lines after treatment with Trametinib or/and Baricitinib for 24h. Values represent $2^{-\Delta Cq}$ relative to *CIORF43*. n=3 independent biological replicates. Means \pm S.D. are shown. Significance was assessed using Two-way ANOVA and indicated as follows: ns $p > 0.05$.

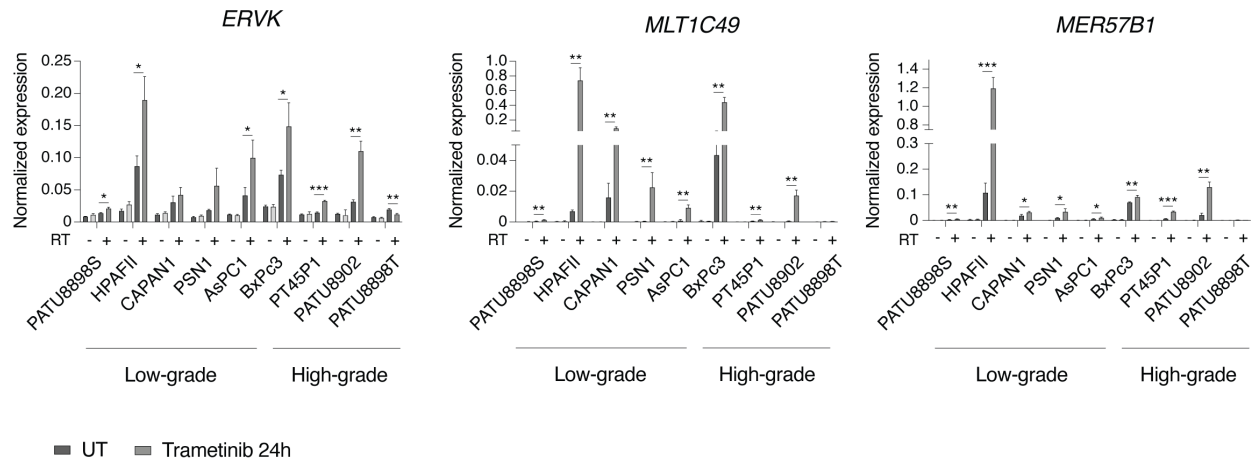


Figure S4. Induction of LTR repeats in a panel of PDAC cell lines.

RT-qPCR analysis of selected ERVs in a panel of human PDAC cell lines after treatment with Trametinib or vehicle for 24h. Values represent $2^{-\Delta Cq}$ relative to *CIORF43*. $n=3$ independent biological replicates. Means \pm SD are shown. Significance was assessed using T-test and indicated as follows: * $p \leq 0.05$, ** $p \leq 0.01$, *** $p \leq 0.001$. Reverse transcriptase (RT)-minus controls are shown to exclude amplification of repeats from genomic DNA.

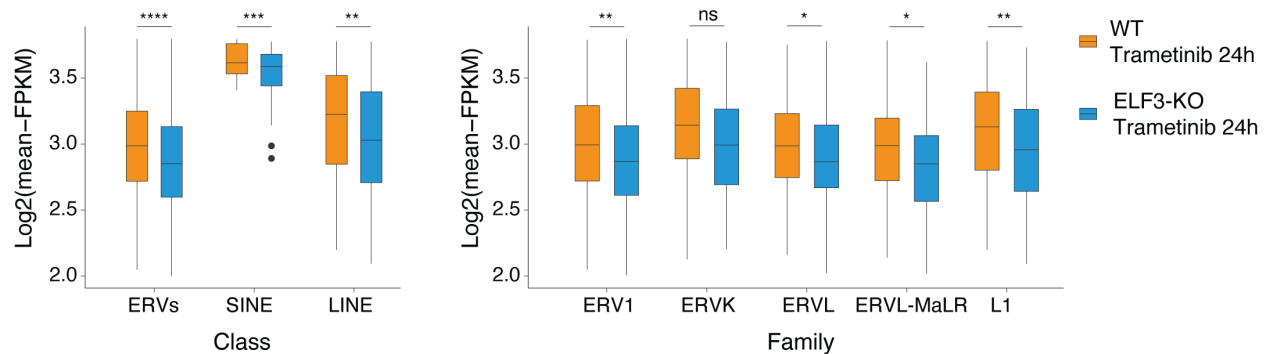


Figure S5. Abundance of retroelement-derived RNAs in *ELF3*-null cells.

The abundance of the RNAs derived from the indicated retroelements was measured in RNA-seq data from wild type and *ELF3*-null CFPAC1 cells after treatment with Trametinib for 24h. Significance was assessed using Wilcoxon Test and indicated as follows: ns $p > 0.05$, * $p \leq 0.05$, ** $p \leq 0.01$, *** $p \leq 0.001$, **** $p \leq 0.0001$.

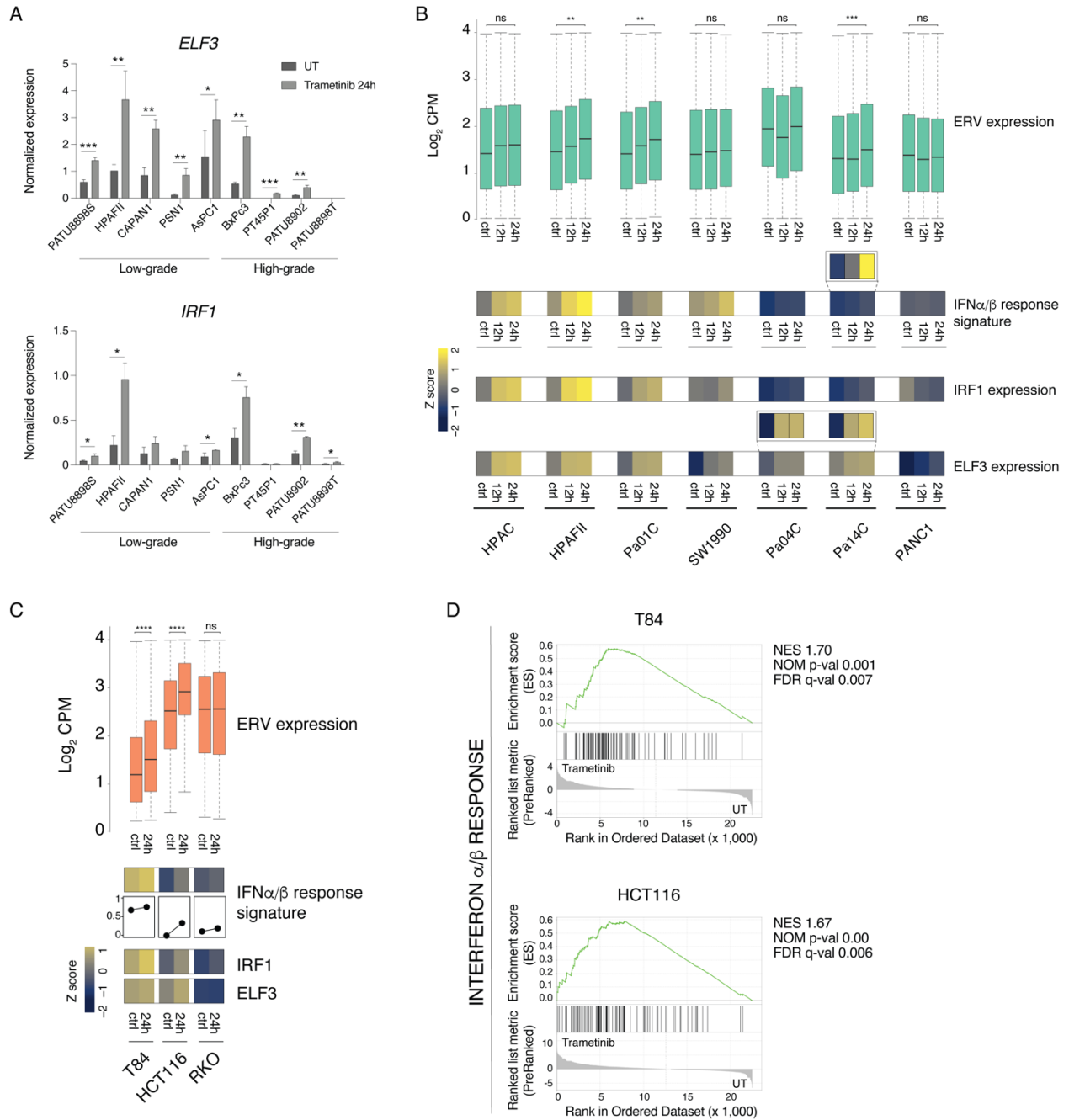


Figure S6. Activation of the *ELF3-IRF1-ERV* pathway and induction of the *IFN* response in PDAC and colon cancer cell models.

A) RT-qPCR analysis of *ELF3* and *IRF1* genes in a broad panel of human PDAC cell lines after treatment with Trametinib or vehicle for 24h. Values represent $2^{-\Delta\Delta Cq}$ relative to *CIORF43*. $n=3$ independent biological replicates. Means \pm SD are shown. Significance was assessed using T-test and indicated as follows: * $p \leq 0.05$, ** $p \leq 0.01$, *** $p \leq 0.001$.

B) *ELF3-IRF1-ERV-IFN* pathway activation in several PDAC cell lines treated with the ERK1/2 inhibitor SCH772984.

Top panel: Box plots showing repetitive elements abundances in PDAC cell lines (17) after ERK inhibitor treatment. Long terminal repeat (LTR) elements including ERVs families were shown. Two-sided Wilcoxon rank-sum tests (24h of treatment versus control) are shown. ns $p > 0.05$, * $p \leq 0.05$, ** $p \leq 0.01$, *** $p \leq 0.001$. Bottom panel: Heatmap of IFN response gene signature score generated by ssGSEA in PDAC cell lines (17) after ERK inhibitor treatment. RNA-seq normalized counts are shown as row z-scores. Inserts showing row z-scores computed independently from selected cell lines.

C) ELF3-IRF1-ERV-IFN pathway activation in colon cancer cell lines treated with Trametinib.

Top panel: Box plots showing repetitive elements abundances in colon cancer cell lines (103-105) treated with Trametinib for 24h. Long terminal repeat (LTR) elements including ERVs families are shown. Two-sided Wilcoxon rank-sum tests (24h of treatment versus control) are shown. ns $p > 0.05$, * $p \leq 0.05$, ** $p \leq 0.01$, *** $p \leq 0.001$, **** $p \leq 0.0001$. Bottom panel: Heatmap of IFN response gene signature score, and *IRF1* and *ELF3* gene expression in colon cancer cell lines (103-105) after Trametinib treatment. RNA-seq normalized counts are shown as row z-scores. The line annotation shows the normalized expression of IFN response gene signature scores as single data points per sample connected by a segment.

D) GSEA plots showing the differential enrichment of the type I IFN signature in two colon cancer cell lines (104-105) treated with Trametinib for 24h vs. untreated cells.

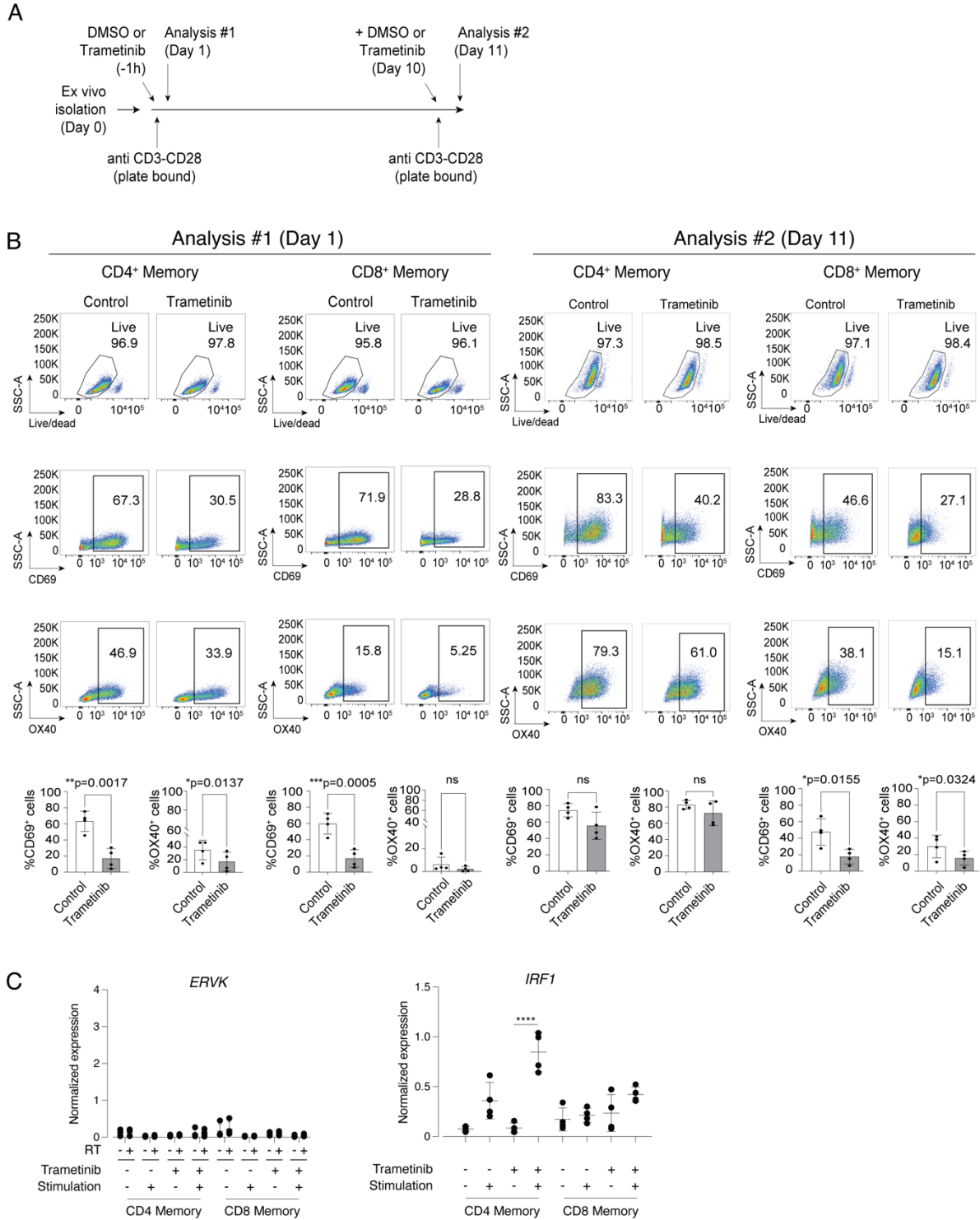


Figure S7. Effects of Trametinib treatment on the activation of primary human T lymphocytes.

A) Schematic representation of the experimental setup. Primary human memory T lymphocytes were treated with Trametinib or vehicle for 24 hours in the presence or

absence of stimulation with plate-bound anti-CD3 and anti-CD28 antibodies, at day 0 and day 10 after ex vivo isolation.

B) Representative FACS plot of n=4 different experiments. Upper plots: Cell viability of CD4⁺ and CD8⁺ memory T lymphocytes treated with Trametinib or vehicle was measured using a live/dead fluorescent dye. Middle and bottom plots: among viable cells, activation of T cells was monitored using surface staining for CD69 and OX40, respectively. The histograms at the bottom show the percentages of positive cells for the different markers. Each dot represents one donor. Means ± SD. Paired t-test, two tailed. Significance was assessed using T-test and indicated as follows: ns p>0.05, * p≤0.05, **p≤0.01, ***p≤0.001.

C) RT-qPCR analysis of *ERVK* and *IRF1* expression in human CD8⁺ and CD4⁺ T lymphocytes after treatment with Trametinib or vehicle for 24h in unstimulated or stimulated conditions. Values represent 2-ΔCq relative to the reference gene (*UBE2D2*). n=4 different donors. Means ± SD are shown. Significance was assessed using One-way ANOVA and indicated as follows: **** p≤0.0001. Reverse transcriptase (RT)-minus controls are shown to exclude amplification of repeats in genomic DNA.

Table S1. *RNA-seq data-sets in Trametinib-treated PDAC cell lines.* Read counts, statistical significance and fold change are shown for each expressed gene in the four cell lines tested. Each sheet contains data for a single cell line.

Table S2. *Genes concordantly regulated by Trametinib across multiple PDAC cell lines.*

Table S3. *Gene Set Enrichment Analysis (GSEA) in individual Trametinib-treated PDAC cells lines.* Upregulated and downregulated signatures are reported separately.

Table S4. *Repeat elements induced by Trametinib in individual cell lines.*

Table S5. *L/H ratios for differentially modified histone peptides Trametinib-treated CFPAC1 cells.*

Table S6. *Genomic data sets used in this study and their GEO identifiers*